纳米晶 LaCo$_x$Fe$_{1-x}$O$_3$ 的合成、表征及湿敏特性

王竹仪   陈 骋   冯彩慧   王金兴   邹 博   赵 萌   吴凤清 *

(吉林大学化学学院, 长春   130023)

摘要： 采用 PEG 溶胶-凝胶法合成了纳米晶 LaCo$_x$Fe$_{1-x}$O$_3$, 并用 DTA-TGA、XRD 以及 SEM 对样品进行表征. 结果表明, 所有样品的原粉在 600 ℃ 焙烧下都形成了稳定的钙钛矿纳米晶, Co 含量对形成纳米晶的固相反应和纳米晶的平均粒子尺寸都有明显的影响. 此外, 还研究了纳米晶 LaCo$_x$Fe$_{1-x}$O$_3$ 的湿敏特性, 发现在所有的样品中, LaCo$_{0.3}$Fe$_{0.7}$O$_3$ 表现出比其它样品好的湿敏特性, 但是此材料只在相对湿度(RH)大于 54%时对湿度的变化有较高的灵敏度, 掺杂适量的 Na$_2$CO$_3$ 可以改善此材料的湿敏特性, 使它在全程湿度范围(RH 11%−95%)内对湿度变化都有很好的响应.

关键词： 钙钛矿； LaCo$_x$Fe$_{1-x}$O$_3$； 湿敏特性

中图分类号： O648

Synthesis, Characterization and Humidity Sensitive Properties of Nanocrystalline LaCo$_x$Fe$_{1-x}$O$_3$

WANG Zhu-Yi   CHEN Cheng   FENG Cai-Hui   WANG Jin-Xing

ZOU Bo   ZHAO Meng   WU Feng-Qing *

(*College of Chemistry, Jilin University, Changchun   130023, P. R. China*)

Abstract：   The nanocrystalline LaCo$_x$Fe$_{1-x}$O$_3$ with different concentrations of Co was prepared by polyethylene glycol (PEG) sol-gel method and characterized by differential thermal analysis and thermal gravimetric analysis (DTA-TGA), X-ray diffraction (XRD), and scanning electron microscope (SEM). It was found that the crystal structure of perovskite-type could be obtained at 600 ℃, and the concentration of Co had significant effects on the solid-state reaction and the average particle size of the obtained nanocrystals. Furthermore, the humidity-sensitive properties of nanocrystalline LaCo$_x$Fe$_{1-x}$O$_3$ were investigated, and it was found that LaCo$_{0.3}$Fe$_{0.7}$O$_3$ exhibited higher sensitivity to humidity compared with other samples. The addition of Na$_2$CO$_3$ improved the humidity-sensitive properties of this sample, and made its response to humidity good in the whole humidity range of 11%−95% relative humidity (RH).

Key Words： Perovskite； LaCo$_x$Fe$_{1-x}$O$_3$； Humidity sensitive property

Perovskite-type oxides have general formula ABO$_3$, in which A is a rare earth or alkaline earth metal and B is a transition metal, and these oxides are typically *p*-type semiconductors. Their composition can be varied in a wide range by partial substitution of lower valent cation in A or B site yielding additional mobile anion vacancies. Their mixed conductivity caused by both ion and electron migration and their high nonstoichiometric composition form the basis of the applications of this group of materials in these areas, such as electrochemistry[1,2], catalysis[3–5], solid oxide fuel cells[6,7], oxygen separation membranes[8], chemical sensors for the detection of humidity[9], alcohol[10], and gases, such as oxygen[11], hydrocarbon[12], and nitric oxide[13].

Earlier studies reported on perovskite oxide LaCo$_x$Fe$_{1-x}$O$_3$ mainly involved methane oxidation catalysis[14–18], alcohol sensor[19], magnetism[20,21], and reduction properties[22–25]. In this article, we report the preparation, characterization, and humidity-sensitive

properties of this material, and the influence of Na_2CO_3 doping on the humidity-sensitive characteristic of material has also been investigated.

1 Experimental

1.1 Material preparation

Nanocrystalline $LaCo_xFe_{1-x}O_3$ was prepared by polyethylene glycol (PEG) method. The chemicals used for the synthesis were $La(NO_3)_3 \cdot 6H_2O$, $Fe(NO_3)_3 \cdot 9H_2O$, and $Co(NO_3)_2 \cdot 6H_2O$ (AR grade) ; and PEG was used as the dispersant. The sample prepared by this method has homogeneous size distribution. According to the formula $LaCo_xFe_{1-x}O_3$ (x=0.0−1.0), stoichiometric amounts of the metal nitrates were dissolved into deionized water, then the three solutions were mixed together, and an appropriate amount of PEG was added to the mixture solution. The solution was stirred and simultaneously heated at 80 ℃ to evaporate water until a sol was obtained, and further drying process made it into raw powder material. Finally, the powder was calcined at 600 ℃ to obtain perovskite-type nanocrystallite.

1.2 Characterization

The thermal decomposition behaviors of the precursors were examined by differential thermal analysis (DTA) and thermal gravimetric analysis (TGA), using a Shimadzu DTG-60 thermal analyzer. The precursors were heated up to 800 ℃ in air at a scan rate of 10 ℃·min⁻¹. The crystal structure of the samples was examined by X-ray diffraction (XRD) on a Shimadzu XRD-6000 diffractometer with Cu K_α radiation. The current and the voltage during the measurements were 30 mA and 40 kV, respectively. The morphology of the samples was observed using a scanning electron microscope (SEM, JEOL JSM-6700F).

1.3 Sensor fabrication

The mixture of the sample with deionized water was ground in a mortar for 3 h to form a paste, and the paste was then screen-printed on ceramic substrates with interdigitated electrodes to obtain the humidity-sensitive thick films. The prepared films were dried in air. The humidity sensor was fabricated after aging at 100% relative humidity (RH) with a voltage of ac 1 V for 24 h. The structure of the sensor is shown in Fig.1.

2 Results and discussion

2.1 Material characterization

Fig.2 shows the DTA and TGA curves of a precursor for $LaCo_{0.3}Fe_{0.7}O_3$. The DTA curve exhibits two exothermic peaks at 269.6, 305.3 ℃, and a weak exothermic peak at 591.0 ℃. The first exothermic peak at 269.6 ℃ refers to the combustion of the
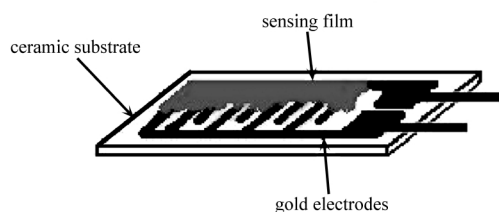

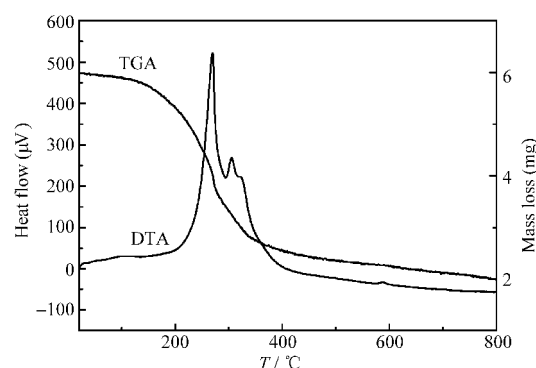**Fig.1   Schematic picture of sensor structure**

Fig.2   DTA/TGA curves of a precursor for $LaCo_{0.3}Fe_{0.7}O_3$

PEG. The second exothermic peak at 305.3 ℃ can be ascribed to the decomposition of the nitrates. Both of the peaks correspond to an appreciable mass loss in the temperature range of 150−350 ℃ in the TGA curve. The weak exothermic peak at 591.0 ℃ may be due to the crystallization because no obvious mass loss is shown in the TGA curve, which is consistent with the following XRD data.

Fig.3 shows the XRD patterns of $LaCo_{0.3}Fe_{0.7}O_3$ calcined at different temperatures for 2 h. It can be noted that after being sintered at 400 or 500 ℃ for 2 h, the powder still remained amorphous. When the sintering temperature was further increased to 600 ℃, the amorphous metal oxide completely transformed to stable perovskite nanocrystallite. With the increase of the calcination temperature, the crystallinity became higher. The regular calcination temperature of the sample used in the following experiments was 600 ℃.

Fig.4 shows the XRD patterns of $LaCo_xFe_{1-x}O_3$ nanocrystallite calcined at 600 ℃ for 2 h. From the results, we can see that the crystal structure of perovskite-type can be obtained in all concentration ranges of Co, and Co can substitute for Fe limitlessly to form $LaCo_xFe_{1-x}O_3$ solid solution. As we know, an ionic radii rule is required to form perovskite structure, i.e., the so-called tolerance factor (f_t) defined by the equation: $f_t=(r_A+r_O)/\sqrt{2(r_B+r_O)}$, where $0.75 < f_t < 1.0$, r_A, r_B, and r_O are the ionic radii of A, B, and the oxygen anion, respectively. Because the ionic radii of Co^{2+} and Fe^{3+} are 0.074 and 0.064 nm, respectively[19], this slight dif-
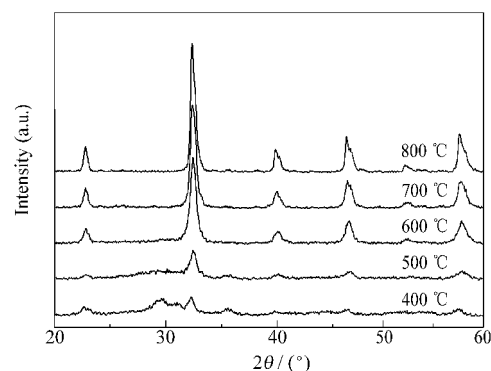

Fig.3   XRD patterns of the $LaCo_{0.3}Fe_{0.7}O_3$ powder
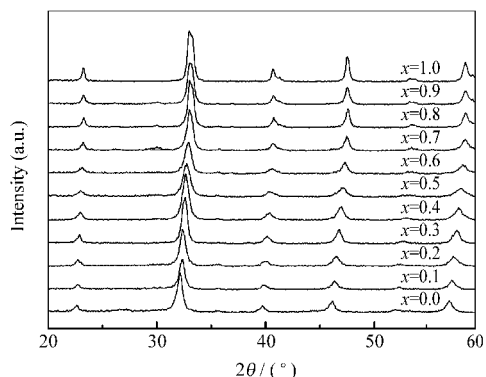**calcined at different temperatures for 2 h**

Fig.4   XRD patterns of LaCo$_x$Fe$_{1-x}$O$_3$ nanocrystallite calcined at 600 ℃ for 2 h

ference makes the perovskite structure to be maintained within tolerance factor.

Table 1 shows the average particle sizes of nanocrystalline LaCo$_x$Fe$_{1-x}$O$_3$ calcined at different temperatures for 2 h. The average particle sizes were determined by the Scherrer equation. It can be found that after forming the stable perovskite structure, the particle sizes increased with further increasing the calcination temperature. The concentration of Co had remarkable effects on the average particle size of nanocrystallite, the particle size initially decreased, then increased with the increase in concentration of Co under the same calcination temperature, and the particle size was the smallest when *x* was 0.5. This trend was more obvious especially after the temperature was increased to 800 ℃. It was supposed that the behavior was caused by enhancing lattice defect. Because the valence of Co^{2+} is lower than that of Fe^{3+}, when the trivalent Fe^{3+} ions in LaFeO$_3$ were replaced by divalent Co^{2+} to form LaCo$_x$Fe$_{1-x}$O$_3$, the charge neutrality was maintained by the formation of oxygen vacancies or the valence change of transition metal ions (like Fe^{4+}/Fe^{3+} or Co^{3+}/Co^{2+}). Therefore, the oxide had an oxygen deficiency due to the high oxygen vacancy concentration. The presence of the large oxygen vacancies may distort the lattice structure of perovskite slightly, and restrain the growth of nanoparticles. When the mole concentration of Co was equal to that of Fe, crystallinity was the smallest. The defect was increasing and the growth of crystalline grains was restrained.

The SEM micrograph (Fig.5) of LaCo$_{0.3}$Fe$_{0.7}$O$_3$ calcined at 600 ℃ exhibited slight crystallite agglomeration. The nanoporous structure of the sample was likely to facilitate the adsorption of water molecules.

Table 1   Particle sizes of LaCo$_x$Fe$_{1-x}$O$_3$ calcined at different temperatures for 2 h

T/℃	x										
	0.0	0.1	0.2	0.3	0.4	0.5	0.6	0.7	0.8	0.9	1.0
	Particle size (nm)										
600	14.9	14.8	13.5	11.7	11.4	10.2	11.4	11.5	11.6	11.8	15.1
700	21.7	20.5	18.1	13.9	11.7	10.5	11.8	12.1	12.3	12.9	35.3
800	34.9	27.7	26.7	17.4	15.8	10.5	26.7	29.2	41.5	41.9	50.8
850	50.1	31.6	30.6	26.3	25.6	10.6	28.3	30.1	43.6	47.2	58.9

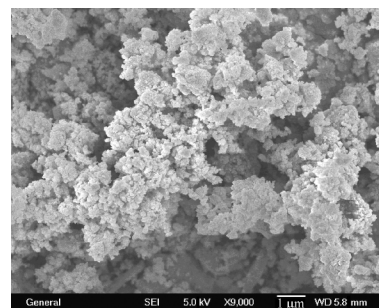**Fig.5   SEM micrograph of LaCo$_{0.3}$Fe$_{0.7}$O$_3$ calcined at 600 ℃ for 2 h**

2.2   Humidity-sensitive properties of the samples

Fig.6 shows the humidity response of LaCo$_x$Fe$_{1-x}$O$_3$. The applied working voltage was 1 V, and the temperature was maintained at ca 20 ℃. It was found that LaCo$_x$Fe$_{1-x}$O$_3$ (*x*=0.0, 0.1, 0.2, 0.3, 0.4) showed sensitivity to humidity in the relative humidity (RH) above 54%; and LaCo$_x$Fe$_{1-x}$O$_3$ (*x*=0.5, 0.6, 0.7) only showed sensitivity to humidity in the RH above 75%; when *x* was 0.8, 0.9, and 1.0, the samples became insensitive to changes in humidity. The sample LaCo$_{0.3}$Fe$_{0.7}$O$_3$ showed the highest sensitivity to changes in humidity when compared with the other samples, so it was chosen for further experiments.

To improve the humidity-sensitive properties of this material, the doping of the monobasic alkali cation was considered. The dependence of resistance *R* on the RH shown in Fig.7 was mea-
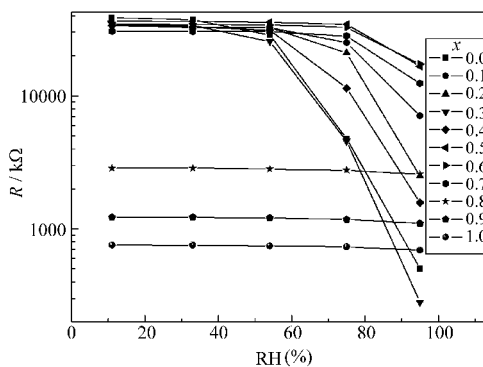

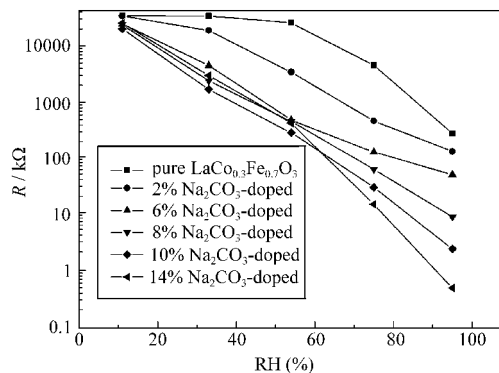**Fig.6   Dependence of resistance on the RH for LaCo$_x$Fe$_{1-x}$O$_3$ measured at 100 Hz**

Fig.7   RH dependence of resistance for pure and Na$_2$CO$_3$-doped LaCo$_{0.3}$Fe$_{0.7}$O$_3$ at 100 Hz

sured for pure and Na$_2$CO$_3$-doped LaCo$_{0.3}$Fe$_{0.7}$O$_3$ at ca 20 ℃. From the results, it was found that Na$_2$CO$_3$ doping improved the sensitivity of the sample in the low humidity range of 11%−54% RH significantly. The response of the samples with Na$_2$CO$_3$ doping of 8% (*w*, mass fraction) or 10% (*w*) to humidity was linear in the entire humidity range tested (11%−95% RH), exhibiting a good exponential relationship, a resistance variation of four orders of magnitude was obtained. Further increase in doping up to 14% (*w*) enhanced the sensitivity but caused the poor linear behavior, which cannot be used for sensor purposes.

3   Conclusions

The nanocrystalline LaCo$_x$Fe$_{1-x}$O$_3$ was prepared by PEG sol-gel method, and the crystal structure of perovskite-type could be obtained at the calcination temperature of 600 ℃. The average particle size of LaCo$_x$Fe$_{1-x}$O$_3$ nanocrystals increased with the increase in the calcination temperature, but when the calcination temperature was of the same condition, the average particle size of nanocrystals initially decreased, and then increased with the increase in the concentration of Co, and the particle size had the minimum when *x* was 0.5. It was supposed that the behavior was caused by enhancing lattice defect.

The investigation of the humidity-sensitive characteristic of nanocrystalline LaCo$_x$Fe$_{1-x}$O$_3$ thick film sensor showed that LaCo$_{0.3}$Fe$_{0.7}$O$_3$ exhibited the higher sensitivity to humidity compared with the other samples. But it only showed sensitivity to humidity in the RH above 54%. The addition of Na$_2$CO$_3$ improved its sensitivity and increased the response to humidity in the entire humidity range of 11%−95% RH.

References

1   Bi, Z. H.; Cheng, M. J.; Dong, Y. L.; Wu, H. J.; She, Y. C.; Yi, B. L. *Solid State Ionics,* **2005, 176**(7−8): 655

2   Kharton, V. V.; Yaremchenko, A. A.; Naumovich, E. N. *J. Solid State Electrochem.,* **1999, 3**(6): 303

3   Tao, S. W.; Irvine, J. T. S. *Chem. Mater.,* **2004, 16**(21): 4116

4   Leontiou, A. A.; Ladavos, A. K.; Pomonis, P. J. *Applied Catalysis A*: *General,* **2003, 241**(1−2): 133

5   Liu, Y.; Meng, M.; Yao, J. S.; Zha, Y. Q. *Acta Phys. -Chim. Sin.,* **2007, 23**(5): 641 [刘　咏, 孟　明, 姚金松, 查宇清. 物理化学学报, **2007, 23**(5): 641]

6   Skinner, S. J. *Fuel Cells Bulletin,* **2001, 4**(33): 6

7   Uhlenbruck, S.; Tietz, F. *Materials Science and Engineering B,* **2004, 107**(3): 277

8   Takamura, H.; Enomoto, K.; Aizumi, Y.; Kamegawa, A.; Okada, M. *Solid State Ionics,* **2004, 175**(1−4): 379

9   Holc, J.; Slunečko, J.; Hrovat, M. *Sensors and Actuators B*: *Chemical,* **1995, 26**(1−3): 99

10   Kong, L. B.; Shen, Y. S. *Sensors and Actuators B*: *Chemical,* **1996, 30**(3): 217

11   Lukaszewicz, J. P.; Miura, N.; Yamazoe, N. *Sensors and Actuators B*: *Chemical,* **1990, 1**(1−6): 195

12   Brosha, E. L.; Mukundan, R.; Brown, D. R.; Garzon, F. H.; Visser, J. H.; Zanini, M.; Zhou, Z.; Logothetis, E. M. *Sensors and Actuators B*: *Chemical,* **2000, 69**(1−2): 171

13   Traversa, E.; Matsushima, S.; Okada, G.; Sadaoka, Y.; Sakai, Y.; Watanabe, K. *Sensors and Actuators B*: *Chemical,* **1995, 25**(1−3): 661

14   Szabo, V.; Bassir, M.; van Neste, A.; Kaliaguine, S. *Applied Catalysis B*: *Environmental,* **2003, 43**(1): 81

15   Royer, S.; Bérubé, F.; Kaliaguine, S. *Applied Catalysis A*: *General,* **2005, 282**(1−2): 273

16   Royer, S.; Duprez, D.; Kaliaguine, S. *J. Catal.,* **2005, 234**(2): 364

17   Royer, S.; van Neste, A.; Davidson, R.; McIntyre, S.; Kaliaguine, S. *Ind. Eng. Chem. Res.,* **2004, 43**(18): 5670

18   Goldwasser, M. R.; Rivas, M. E.; Lugo, M. L.; Pietri, E.; Pérez-Zurita, J.; Cubeiro, M. L.; Griboval-Constant, A.; Leclercq, G. *Catal. Today,* **2005, 107−108**: 106

19   Ge, X. T.; Liu, Y. F.; Liu, X. Q. *Sensors and Actuators B*: *Chemical,* **2001, 79**(2−3): 171

20   Troyanchuk, I. O.; Karpinskiǐ, D. V.; Dobryanskiǐ, V. M.; Fedotova, Y. A.; Szymczak, H. *Journal of Experimental and Theoretical Physics,* **2005, 100**(6): 1121

21   Karpinsky, D. V.; Troyanchuk, I. O.; Bärner, K.; Szymczak, H.; Tovar, M. *Journal of Physics*: *Condensed Matter,* **2005, 17**(46): 7219

22   Berry, F. J.; Gancedo, J. R.; Marco, J. F.; Ren, X. L. *J. Solid State Chem.,* **2004, 177**(6): 2101

23   Bedel, L.; Roger, A. C.; Estournes, C.; Kiennemann, A. *Catal. Today,* **2003, 85**(2−4): 207

24   Berry, F. J.; Ren, X. L.; Gancedo, J. R.; Marco, J. F. *Hyperfine Interactions,* **2004, 156/157**: 335

25   Berry, F. J.; Ren, X.; Marco, J. F. *Czechoslovak Journal of Physics,* **2005, 55**(7): 771